Chemistry–A European Journal

Research Article
doi.org/10.1002/chem.202500702

Chemistry Europe
European Chemical Societies Publishing

www.chemeurj.org

Total Synthesis of the Membrane Spanning Tetraether Lipid brGDGT Ia and Elucidation of Its Stereochemical Configuration

Samarpita Mahapatra,[a] Sebastian H. Kopf,[b] Toby Halamka,[c] Christian Merten,[d] Deborah A. Drost,[d] and Adriaan J. Minnaard*[a]

Glycerol dialkyl glycerol tetraethers (GDGTs) are a group of membrane spanning lipids produced by both Archaea and Bacteria. Branched GDGTs (brGDGTs) are a class of these tetraether lipids known to be produced by certain bacteria and are commonly found in terrestrial environments. Due to their environmental ubiquity, high preservation potential, and role in membrane adaptation, brGDGTs form the basis of many widely employed paleoenvironmental proxies. The tetramethylated brGDGT Ia is the most commonly reported branched tetraether in cultured *Acidobacteria* and is a key component of brGDGT-based temperature indices. Herein, we report the first total synthesis of brGDGT Ia, thereby elucidating the relative configuration of the methyl branches as syn. We further demonstrate that VCD spectroscopy is a suitable tool to determine the absolute configuration of these cryptochiral compounds, a method waiting to be applied to the natural lipid, but currently hampered by its limited availability.

1. Introduction

Life on Earth has been classified into three main domains—Archaea, Bacteria, and Eukarya—on the basis of their phylogenetic information which deals with the evolutionary history and diversity of these organisms.[1,2] In addition to differences in ribosomal RNA, the lipid architecture of archaeal membranes differentiates this domain from those of Bacteria and Eukarya. Archaeal lipids are comprised of isoprenoid alkyl chains, whereas bacterial and eukaryotic lipids have fatty acid chains (Figure 1A,B).[3] Furthermore, the hydrocarbon chains in Archaea are attached via ether bonds to the glycerol backbone, whereas in Bacteria and Eukarya this is most commonly through ester bonds.

A significant difference between archaeal lipids and those of Bacteria and Eukarya is the opposite stereochemistry of their glycerol backbone, which is *sn*-glycerol-1-phosphate for archaeal lipids and *sn*-glycerol-3-phosphate for bacterial (and eukaryal) lipids.[4,5] This description of the glycerol backbone in lipids is according to the "*sn*, that is, stereospecific numbering" of glycerol (Figure 1C).[6] The numbering is based on the arrangement of the phosphate group with respect to the hydroxy group on the second carbon of glycerol. The fundamental differences between the unique lipid structures of Archaea and the shared structural attributes of bacterial and eukaryotic lipids forms the basis of the so-called "lipid divide". Archaea and Bacteria are assumed to have arisen from a common ancestor whose membrane comprised a mixed lipid structure. This lipid divide is important for geochemists and biologists in the search to understand the evolutionary pressure for segregation of the lipid structures between Archaea, Bacteria, and Eukarya.[7–9] Archaeal membrane lipids can occur as glycerol diethers (e.g., Archaeol; Figure 1A) and also as membrane spanning tetraethers, named glycerol dialkyl glycerol tetraethers (GDGTs). The isoprenoidal methyl branches in the alkyl chains of these lipids provide fluidity and decrease the permeability of the membrane, whereas the ether bonds increase resistance to hydrolysis. These features are thought to help Archaea survive under extreme temperature, pH, and salinity conditions.[10]

In 2000, Sinninghe Damsté et al. discovered an unprecedented class of GDGTs in samples of the Holocene Bargerveen peat bog in SE Drenthe, The Netherlands.[11] The extracted lipids were analyzed with HPLC-MS, where the total ion chromatogram showed unknown components along with ions characteristic to loss of water and a glycerol moiety. This suggested the unknown components to be GDGTs. The ^{1}H and ^{13}C NMR analysis of the lipids showed similarity with the signals of archaeal GDGTs, especially the ^{13}C shifts of the glycerol moiety and the ether-bound methylene units in the alkyl chain. Thereby confirming the presence of ether-bound glycerol moieties in the extracted lipids. Until then, some hyperthermophilic and anaerobic bacteria were known to produce branched mono and diether lipids, but no tetraether lipids.[12] The structural resemblance of the discovered tetraethers with archaeal GDGTs and bacterial branched lipids led to the classification of the new

[a] S. Mahapatra, A. J. Minnaard
Stratingh Institute for Chemistry, University of Groningen, Nijenborgh 7, Groningen 9747 AG, The Netherlands
E-mail: a.j.minnaard@rug.nl

[b] S. H. Kopf
Department of Geological Sciences, University of Colorado Boulder, Denver, CO, USA

[c] T. Halamka
Organic Geochemistry Unit, School of Chemistry, University of Bristol, Bristol BS8 1TS, UK

[d] C. Merten, D. A. Drost
Organic Chemistry II, Ruhr University Bochum, Bochum, Germany

Supporting information for this article is available on the WWW under https://doi.org/10.1002/chem.202500702

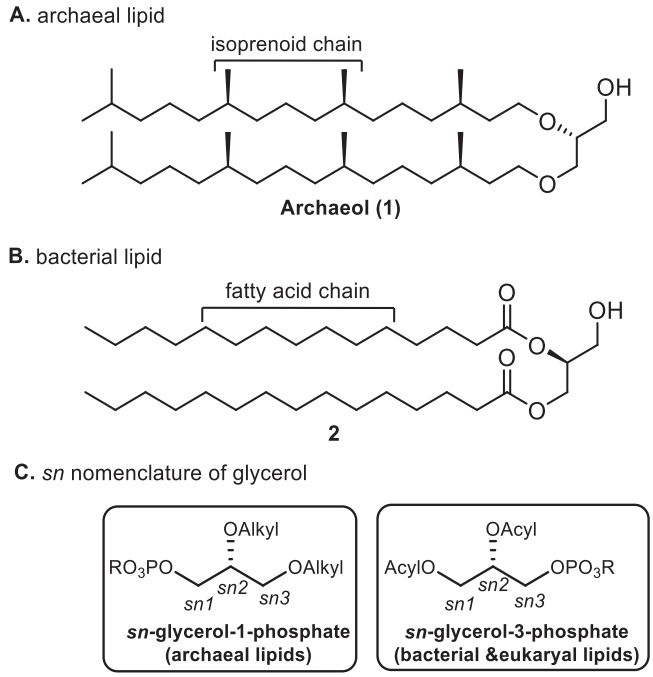

Figure 1. The overall structure of (A) archaeal lipids; (B) bacterial lipids; (C) "*sn*" configuration of glycerol.

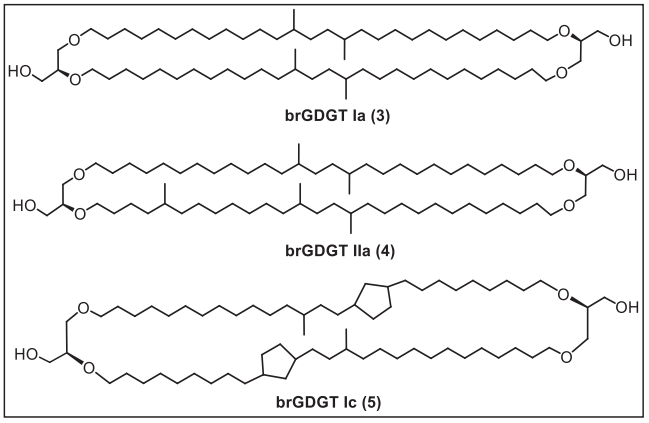

Figure 2. Representative examples of brGDGTs.

compounds as branched glycerol dialkyl glycerol tetraethers (brGDGTs).

The biosynthesis of GDGTs has gained attention worldwide and is a continuing line of research. In archaeal GDGTs, the methyl branches arise from the isoprenoidal structure of the phytanyl chain, while in contrast, the methyl branches in branched GDGTs likely arise from the coupling of fatty acid chains having an isopropyl group at their terminus. Archaeal GDGTs are formed via a radical enzyme mechanism that facilitates the Csp^3–Csp^3 coupling of two Archaeol lipids.[13] In recent studies, it has been found that a radical (*S*)-adenosylmethionine (SAM) enzyme (tetraether synthase [Tes]) is involved in the tail-to-tail radical coupling of two diether lipids in Archaea, resulting in the corresponding archaeal GDGT.[13,14] Glycerol mono- and di-ether lipids containing isopentadecane (commonly denoted as *iso*-C15:0) alkyl components and the most likely derived 13,16 dimethyl octacosanedioic acids (*iso*-diabolic acid)[15] have been identified in several bacterial species, some of which have been shown to produce branched tetraethers. Additionally, ^{13}C-labeled leucine was used to demonstrate the uptake of *iso*-branched fatty acids in the production of *iso*-Diabolic acid-bearing lipids in the bacterium *Thermoanaerobacter ethanolicus*.[16] This provides evidence for the tail-to-tail coupling in the biosynthesis of branched GDGTs (e.g., brGDGT Ia; Figure 2). Another structural feature of some branched GDGTs is the occurrence of additional methyl branches on the alkyl chain (e.g., brGDGT IIa; Figure 2). Whereas a tail-to-tail radical coupling pathway provides a plausible explanation for the 1,4-methyl branching in branched GDGTs, the presence of additional methyl substituents at several positions on the fatty acid chain remains unexplained.

Pinning down a source organism of the branched tetraethers was challenging, however, due to the vast diversity of microorganisms in peats and the apparent combination of archaeal and bacterial traits observed in these lipids.[17] A stereochemical examination of the glycerol backbone using Mosher's ester was performed and the glycerol configuration of a bacterial lipid, rather than an archaeal lipid, was shown.[12] En route to the identification of the bacteria producing these lipids, a comparison was made between the microbial 16s rRNA genes and the archaeal and bacterial lipids obtained from another peat bog, the Saxnäs Mosse peat bog, in Sweden.[18,19] This revealed the abundant presence of *Acidobacteria*, a highly diverse phylum of Bacteria that are globally abundant in soils.

Over the years, *Acidobacteria* have emerged as a focus of the search for brGDGT-producing organisms due to their environmental correlations with these tetraether lipids and the abundance of *iso*-diabolic acid found in lipid extracts of cultured members of the phylum.[15] At present, all known producers of brGDGTs in microbial culture are members of the *Acidobacteria*[15,20,21] but whether that is the case in nature is difficult to study without the complete resolution of the biosynthetic pathway of these enigmatic lipids. Progress in this field is in part hampered by the lack of synthetic intermediates and authentic standards. This limits the ability to conduct biochemical experiments and quantitative analyses affecting all disciplines of GDGT work, including the application of GDGTs to paleoenvironmental reconstructions.[22–26] While many GDGT-based proxies are semi-quantitative or based on ratios of structurally similar compounds (i.e., the sea surface temperature proxy TEX_{86}[27] is based on ratios of archaeal GDGTs and the soil temperature proxy MBT, methylation of branched tetraethers[28] is based on ratios of bacterial GDGTs), certain applications of GDGTs rely on the direct comparison of archaeal and bacterial GDGTs. Without synthetic standards, such analyses, like the widely employed BIT index,[29] are particularly susceptible to errors derived from differences in the ionization efficiency of the two different classes of GDGTs and subsequent intra-lab discrepancies.[30] Our group has previously described the preparation of some archaeal GDGTs but the need for bacterial GDGTs remains.

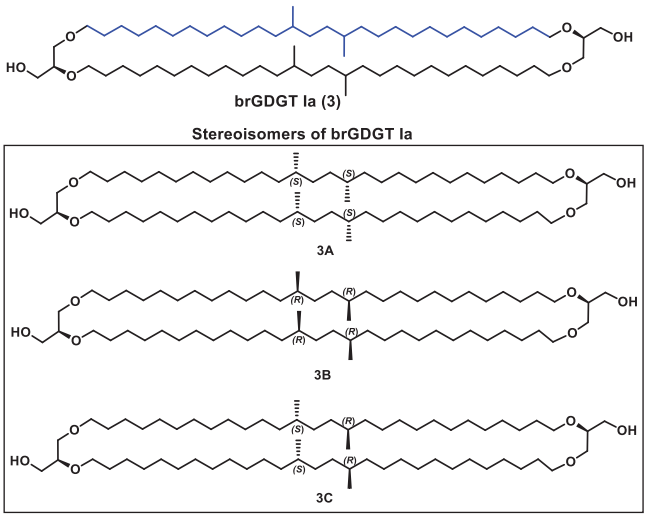

Figure 3. Syn- and anti-stereoisomers of the tetramethyl lipid brGDGT Ia **3**.

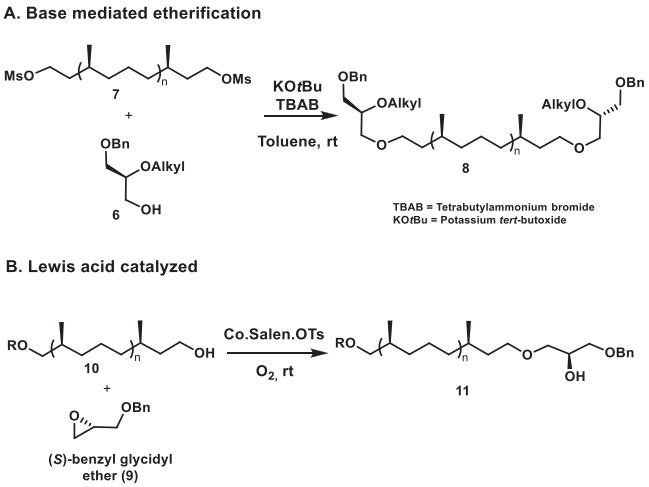

Scheme 1. Overview of strategies for connection of hydrocarbon chain to glycerol fragment.

1.1. Structure and Stereochemistry of brGDGTs

The hydrocarbon chains of brGDGTs are connected in an anti-parallel arrangement to the glycerol backbone, that is, one side is attached to the secondary position of the glycerol and the other side to the primary position.[31] Unlike the co-existing archaeal lipids caldarchaeol, with an anti-parallel arrangement, and its counterpart iso-caldarchaeol, with a parallel arrangement of the chains,[32,33] brGDGTs occur predominantly in the anti-parallel arrangement. There are no prior reports on the synthesis of brGDGTs and the stereochemistry of their methyl branches has not been determined. Although they have structural similarities with archaeal GDGTs, the absence of the isoprenoid structure as in Archaea and the methyl branches being distant from the glycerol backbone (known stereochemistry), makes it challenging to elucidate the stereochemistry of the methyl groups. As brGDGTs are unique in their structure, a comparison with lipids of known stereochemistry is also not possible.

From a stereochemical point of view, **3** is very interesting (Figure 3). Just focusing on the hydrocarbon chain containing the methyl branches, so 13,16-dimethyl octacosane (highlighted in blue in Figure 3), an anti-relationship of the methyl substituents would result in a meso-compound, whereas a syn-relationship would result in two possible enantiomers (i.e., *S*,*S* and *R*,*R*). Considering the whole molecule **3**, this potential "meso-character" of the hydrocarbon chains would de jure disappear, as the termini of the chains differ. De facto, however, the differences are so small and the termini are so far away from the methyl substituents that there might not be any noticeable optical activity and detectable chromatographic separation. One might conclude that the molecule is crypto-optically active ("cryptochiral") in this respect.[34]

We decided to take up the challenge to determine the stereochemical configuration of the methyl branches by carrying out the synthesis of the syn-stereoisomers **3A** and **3B** (Figure 3) and anti-stereoisomer **3C** of the tetramethyl lipid brGDGT Ia (**3**) and compare these synthetic stereoisomers with **3** obtained from a natural extract. Considering the cryptochiral behavior of **3**, a direct comparison of synthetic and natural **3** would, however, be difficult and potentially inconclusive. Therefore, we initially aimed for a comparison of the corresponding 13,16-dimethyl octacosane isomers. This would comprise the degradation of the natural material to this alkane.

In our group, we previously prepared the archaeal tetraether lipids cyclo-archaeol, caldarchaeol, iso-caldarchaeol,[32] and crenarchaeol.[35] One of the crucial steps used in their synthesis is the connection of the hydrocarbon chain to the glycerol backbone via etherification. In the crenarchaeol synthesis, we selected for this a base-mediated etherification of the glycerol derivative **6** with the mesylate **7** (Scheme 1A). In the synthesis of cyclo-archaeol, caldarchaeol, and iso-caldarchaeol we successfully used the Jacobsen Co-Salen.OTs catalyst as a Lewis acid for epoxide ring opening of **9** with **10** to obtain **11** (Scheme 1B). We planned to use this expertise in the synthesis of **3** as well.

2. Results and Discussion

Considering the methyl-branched stereocenters, a separate synthetic route for both the syn- and the anti-configuration of brGDGT Ia (3) had to be designed. The retrosynthesis for both routes started with the disconnection at the ether bond between the chain and the glycerol fragment. In the retrosynthetic analysis of 3A (and also in the enantiomeric series 3B) (Scheme 2A), the ether bond disconnection provides two intermediates, the aliphatic chain 12 and the glycerol fragment 13. For our synthesis, we chose (*R*)-benzyl glycidyl ether (13) as the glycerol building block, exhibiting the required configuration for the glycerol stereochemistry of a bacterial lipid. The anti-parallel arrangement has to be achieved by a sequential connection of 12 to 13 and a careful selection of protecting groups. 12 can be obtained through olefin metathesis of methyl-branched alkene 14. 14 is the cornerstone of the synthesis as the absolute configuration of the methyl branch determines the stereo-configuration of the whole

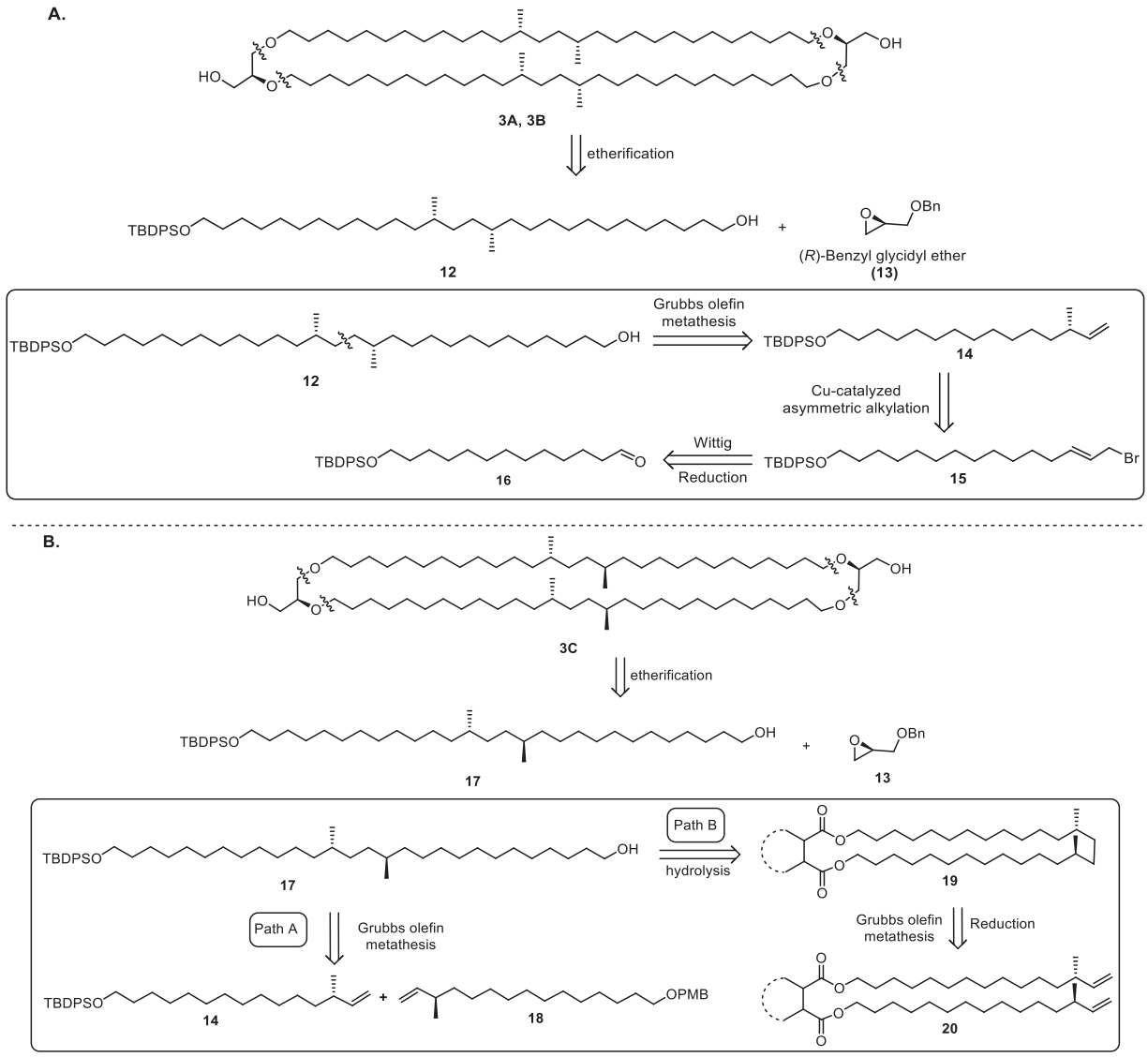

Scheme 2. Retrosynthetic analysis of stereoisomers of brGDGT Ia 3: (A) Stereoisomer 3A (and in the enantiomeric series 3B) and (B) stereoisomer 3C.

lipid. For the enantioselective introduction of this methyl group, we opted to apply a Cu-catalyzed asymmetric alkylation on allyl bromide 15, a method well-developed within the group.[36,37] The allyl bromide 15 was simplified to the aldehyde 16, chosen as the starting point for the synthesis. In the retrosynthesis of the lipid with anti-Me configuration 3C (Scheme 2B), disconnection at the ether bond provided the intermediates aliphatic chain 17 and (*R*)-benzyl glycidyl ether 13. Further disconnection of 17 led to two separate alpha-methyl alkenes 14 and 18 that can be connected by olefin metathesis (Path A). Straightforward dimerization is not an option here as a statistical mixture of homo and heterodimers would be the result. It was envisioned that 17 could be obtained through hydrolysis of macro-dilactone 19 having methyl branches in the anti-configuration (Path B). Macro-dilactone 19 was planned to be obtained by ring-closing metathesis of 20, composed of both enantiomers of the methyl branched alkene. The diester 20 can be obtained by sequential esterification of the selected diacid with both the enantiomers.

2.1. Synthesis of "syn-Dimethyl" 12

The synthesis of 12 was realized in 11 steps commencing from commercially available 1,12-dodecanediol (21) (Scheme 3). Monoprotection of 21 with TBDPSCl followed by oxidation of the free hydroxy group provided corresponding aldehyde 22. A Wittig olefination with methoxymethyltriphenyl phosphonium chloride was performed on 22 and acid hydrolysis of the formed enol ether gave aldehyde 16. A stereoselective Wittig olefination of 16 with methyl (triphenylphosphoranylidene)acetate formed selectively the (*E*)-isomer of α,β-unsaturated ester 23, which is a prerequisite for the planned asymmetric alkylation. Chemoselective reduction of 23 with DIBAL-H, provided allyl alcohol 24 exclusively.[37] Allylic alcohol 24 was converted to allylic bromide 15 via an Appel reaction using NBS (*N*-bromosuccinimide) and PPh_3. As described in the retrosynthesis (Scheme 1A), Cu-catalyzed asymmetric alkylation was performed on 15 using MeMgBr and Taniaphos as the chiral ligand.[36] Since the

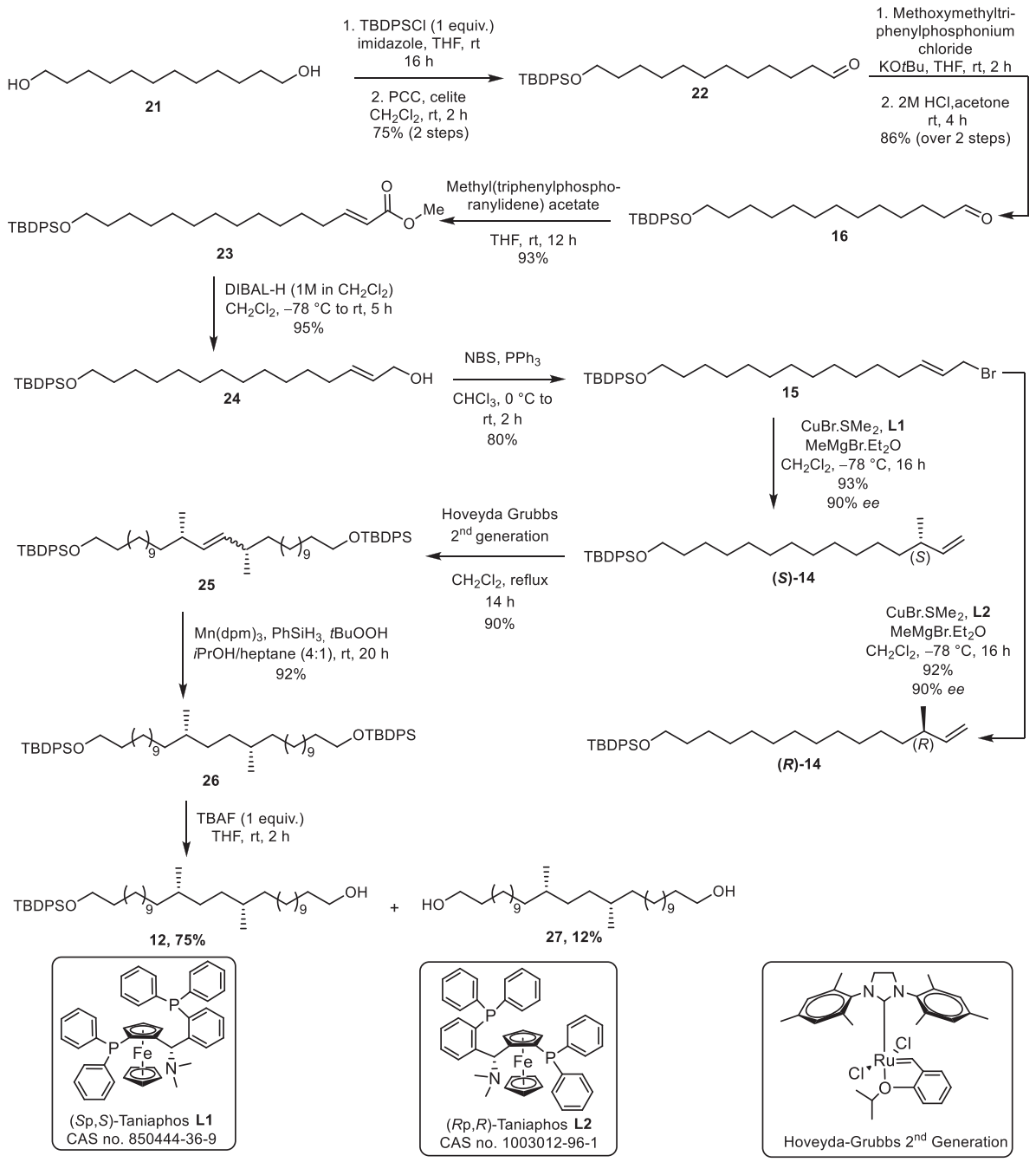

Scheme 3. Synthesis of syn-dimethyl 12.

configuration of the methyl-branched stereocenters in the natural lipid is unknown, we deliberately choose (S_p,*S*)-Taniaphos. To avoid confusion, as has happened in previous reports,[36,38,39] note that this ligand corresponds to CAS No.850444-36-9. The asymmetric alkylation reaction provided alkene 14 in 93% yield. The absolute configuration of the stereocenter was confirmed by carrying out Mosher's ester analysis of the primary alcohol obtained by oxidative cleavage of alkene 14, followed by reduction of the obtained aldehyde and esterification (see Supporting Information). NMR of the Mosher's esters confirmed the (*S*) configuration of the methyl-branched stereocenter.[40,41] This is in agreement with the literature results on similar but different substrates.[37] In addition, integration of the signals in ^{1}H NMR of the Mosher's esters revealed 90% ee for the reaction (see Supporting Information). Though high, the ee is somewhat lower than observed with substrates with shorter chains. Similarly, the opposite enantiomer of the alkene with (*R*) configuration ((*R*)-14) was synthesized using (R_p,*R*)-Taniaphos, CAS No. 1003012-96-1. Alkene (*S*)-14 was subjected to Grubbs olefin metathesis using Hoveyda–Grubbs second generation catalyst to get the homo-dimer 25 in 90% yield. The 90% ee in the preceding asymmetric alkylation step led to the formation of around 10% of the anti-isomer in the dimerization reaction (observed as small signals in the ^{13}C NMR). This isomer could

not be separated by column chromatography. To saturate the alkene, we chose the $Mn(dpm)_3$ and $PhSiH_3$-based HAT reaction developed by the group of Shenvi,[42] as palladium-catalyzed hydrogenation is known to partially racemize α-stereocenters via alkene isomerization. The product 26 was subjected to desilylation using 1 equivalent of TBAF to provide the mono-desilylated product 12. As the substrate is symmetric, a statistical mixture of both mono- and double desilylated products was obtained. The double de-silylated product 27 served as a reference for analytical studies discussed further on in the paper.

2.2. Assembly of the "syn-Dimethyl" Lipid 3A

We planned to use a regioselective epoxide ring-opening reaction of (*R*)-benzyl glycidyl ether (**13**) with **12** using Co-Salen.OTs as the catalyst.[32] Unexpectedly, in the present case we did not observe the formation of the desired product, and the starting materials were left unreacted. Despite numerous attempts and scrutinizing the starting materials and reagents, the reaction did not take place. We considered different Lewis acids and therefore the reaction was performed with $BF_3.OEt_2$, which led to the formation of the desired product in low yield (≈20%). The main product originated from the rearrangement of the epoxide to the corresponding aldehyde, along with significant amounts of unreacted **12**. Apparently, the opening of the epoxide with **12** is sluggish. We speculate that due to the coiling of the long aliphatic chain, the hydroxy group in **12** is less accessible as a nucleophile. To circumvent this problem, we designed a different approach by switching the reactivity of the substrates, that is, converting the glycerol derivative into the nucleophile and the aliphatic chain into the electrophile. We used this "Umpolung" in the synthesis of the archaeal lipid crenarchaeol.[35]

Adhering to the anti-parallel arrangement of the hydrocarbon chains in **3**, two different glycerol derivatives **28** and **29** were synthesized (Scheme 4). (*R*)-benzyl glycidyl ether (**13**) was used as the substrate for both. To obtain **28**, *p*-methoxybenzyl alcohol was deprotonated with NaH and treated with **13**. This resulted in regioselective opening of the epoxide at the primary position (Scheme 4A). Glycerol derivative **29** was obtained in three steps (Scheme 4B); ring-opening of the epoxide with allyl alcohol/NaH to provide **30**, protection of the formed secondary hydroxy group with PMBCl to give **31** and finally, de-allylation with $Pd(PPh_3)_4$ in presence of *N*,*N*-dimethylbarbituric acid to provide **29** with a free primary hydroxy group.

2.3. Completion of the Total Synthesis of Lipid 3A

The final part of the synthesis started with the etherification of the glycerol derivatives. For this, mesylate **32** was prepared from **12** and used for the etherification of **28** with KO*t*Bu as the base and tetrabutylammonium bromide (TBAB) in toluene (Scheme 5, A).[35] Ether **33** was obtained this way in an acceptable yield of 58%. Under these basic conditions, partial de-silylation of the product was observed, which was inconsequential for the next step. After this success, we proceeded with the attachment of

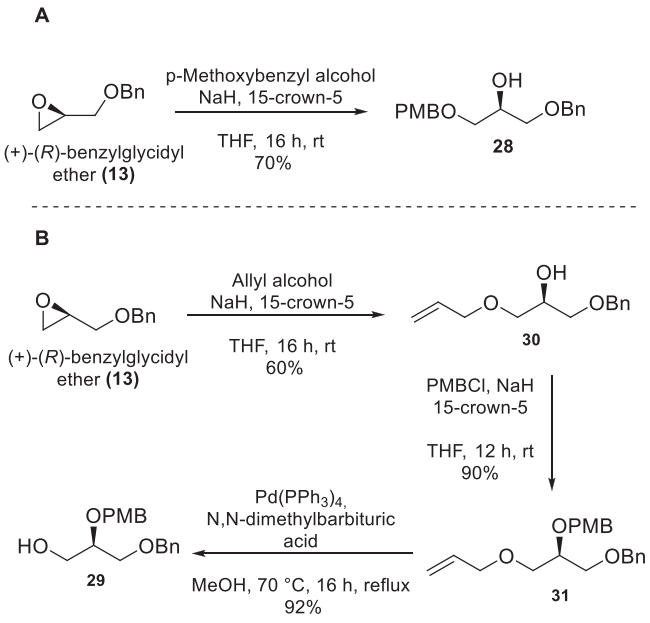

Scheme 4. (A) Synthesis of the glycerol derivative **28**. (B) Synthesis of the glycerol derivative **29**.

the second glycerol backbone through the etherification of **29**. To achieve this, **33** was de-silylated and converted to mesylate **34** followed by treatment with glycerol derivative **29** under the same KO*t*Bu/TBAB conditions. This resulted in the formation of **35** possessing glycerol units at both ends of the chain. Side reactions including elimination and substitution of the mesylate with bromide were also observed, which led to a lower yield of the desired product. Selective removal of the PMB groups in the presence of the benzyl groups was achieved with DDQ in CH_2Cl_2, to obtain diol **36**. The second chain was installed via double alkylation of the free hydroxyl groups in **36** with **37**, followed by a Grubbs ring closing metathesis. The double alkylation of **36** with **37** gave **38** in 73% yield. The unexpected, but welcomed, high yield of this double alkylation compared to the mono-alkylation reactions leading to **33** and **35** was intriguing, also considering the size of **38**. A reason for this could be the use of the mesylate in excess for the double alkylation, which counteracts the effect of the competing side reactions observed previously. Compound **38** was subjected to ring-closing metathesis using Grubbs second-generation catalyst, under high dilution conditions (0.002 M). This led to a highly rewarding 66% yield of the desired macrocycle **39**. The reduction of the alkene with $Mn(dpm)_3$ and $PhSiH_3$ was followed by double de-benzylation with $H_2/Pd(OH)_2$, leading to **3A**.

With 3A in hand, together with an optimized synthesis method, also the other stereoisomer 3B, that is, with the opposite configuration of the methyl branches, was prepared in 12 steps from alkene (*R*)-14 (Scheme 5B), overall yield around 2%. The ^{1}H- and the ^{13}C-NMR spectra of the synthesized stereoisomers 3A/3B matched well with those reported previously by Sinninghe Damsté et al.[11] Interestingly, even though the synthesized lipids are diastereomers, we observed no difference in the signals in the NMR spectra (at 600 MHz for ^{1}H and 125 MHz for ^{13}C).

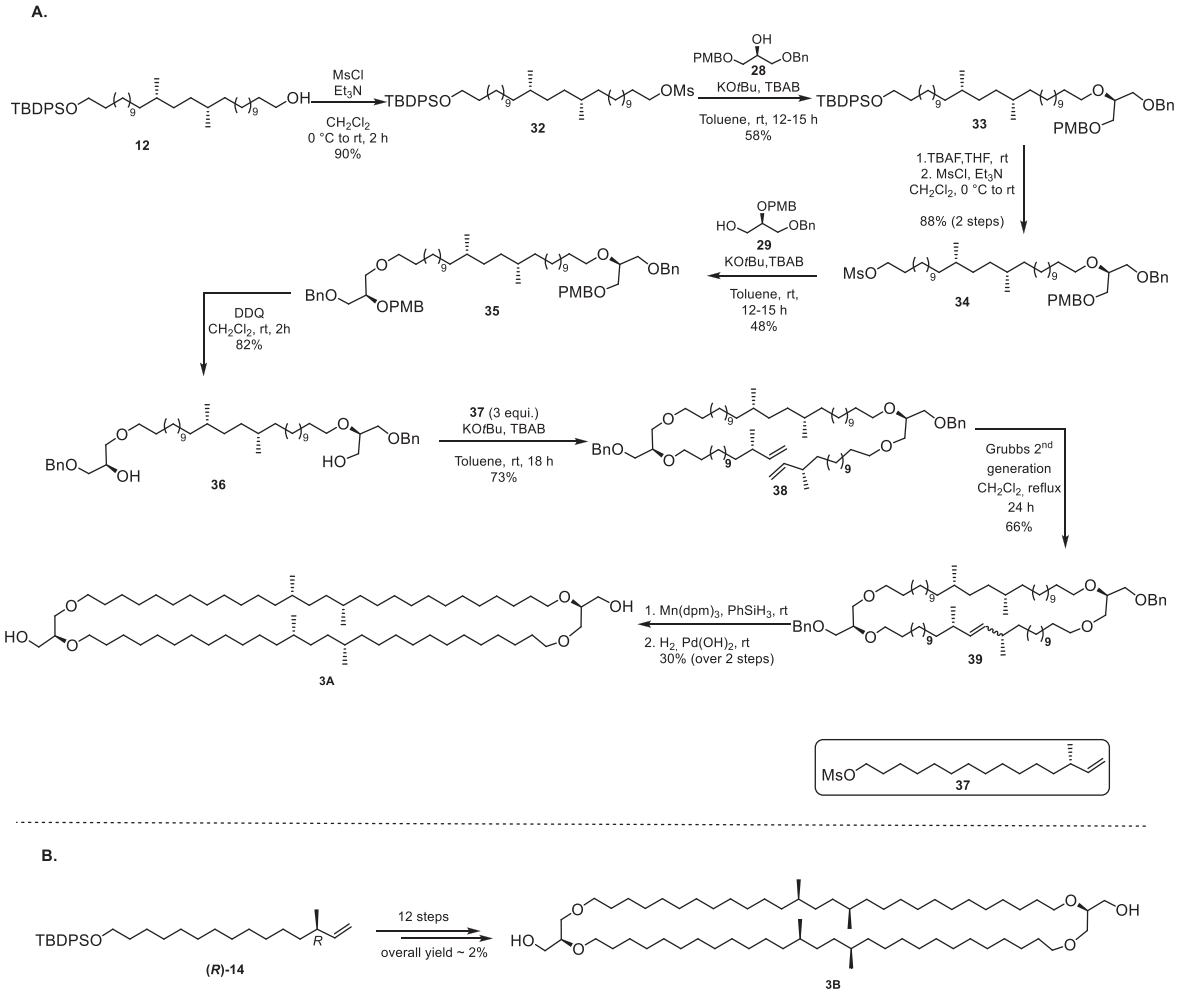

Scheme 5. Synthesis of two stereoisomers of brGDGT Ia 3: (A) 3A and (B) 3B.

2.4. Synthesis of "anti-Dimethyl" 17

With the synthesis of two isomers of the lipid with syn-Me configuration accomplished, we moved on toward the synthesis of brGDGT Ia having an anti-Me configuration, **3C** according to Scheme 2, Path B. The synthesis started by reacting phthalic anhydride **40** with the alkene (***S***)-**41** derived from (***S***)-**14** (see Supporting Information), giving the mono-ester mono-acid **42** (Scheme 6). The second esterification was carried out with (***R***)-**41** (derived from de-silylation of (***R***)-**14**), to obtain diester **43**, a meso-compound. Di-ester **43** was subsequently subjected to ring-closing metathesis using Grubbs second generation catalyst to provide **44**.[32] Reduction of the formed alkene followed by ester hydrolysis provided diol **45** (the diastereomer of diol **27**), with the Me substituents in an anti-configuration. Whereas the ^{1}H NMR spectra of the diols **45** and **27** appeared identical, the ^{13}C NMR spectrum of diol **45** showed small differences in the chemical shift of the methyl carbon and the methine carbon, compared to **27**. In **27**, the chemical shift of the methyl carbon is 19.8 ppm and that of the methine carbon is 37.3 ppm, whereas the same atoms in **45** have chemical shifts of 20.0 and 37.1 ppm, respectively. Although **17** and subsequently lipid **3C** would be accessible following the route developed for **3A** and **3B**, we decided to first study the relative configuration of the methyl-branched stereocenters in natural brGDGT Ia **3** using the prepared fragments.

2.5. Comparison of 13,16-Dimethyloctacosane Derived from Natural 3 with the Synthetic Stereo-Isomers by GC-MS/FID

A direct comparison of the available NMR data of natural brGDGT Ia (**3**)[11] with our synthetic **3A** and **3B** did not provide any solid conclusion, as the spectra appeared identical. Another established strategy in the structure analysis of archaeal lipids is to degrade the lipid by cleaving the ether bonds and convert the chain fragments into their corresponding alkanes. These alkane fragments can then be analyzed with GC-MS. This provides a retention time and a mass fragmentation spectrum. Although we did not expect a significant difference in the mass spectra of the corresponding 13,16-dimethyloctacosanes (**13*S*,16*S*)-46** and (**13*S*,16*R*)-46**, we hoped for a (small) difference in retention time on GC.

Solibacter usitatus strain Ellin6076 grown aerobically at 30 °C, pH 5.5, produces brGDGT Ia (**3**) as its main tetraether lipid.[20,21] An aliquot of the brGDGT Ia extract from *S. usitatus*

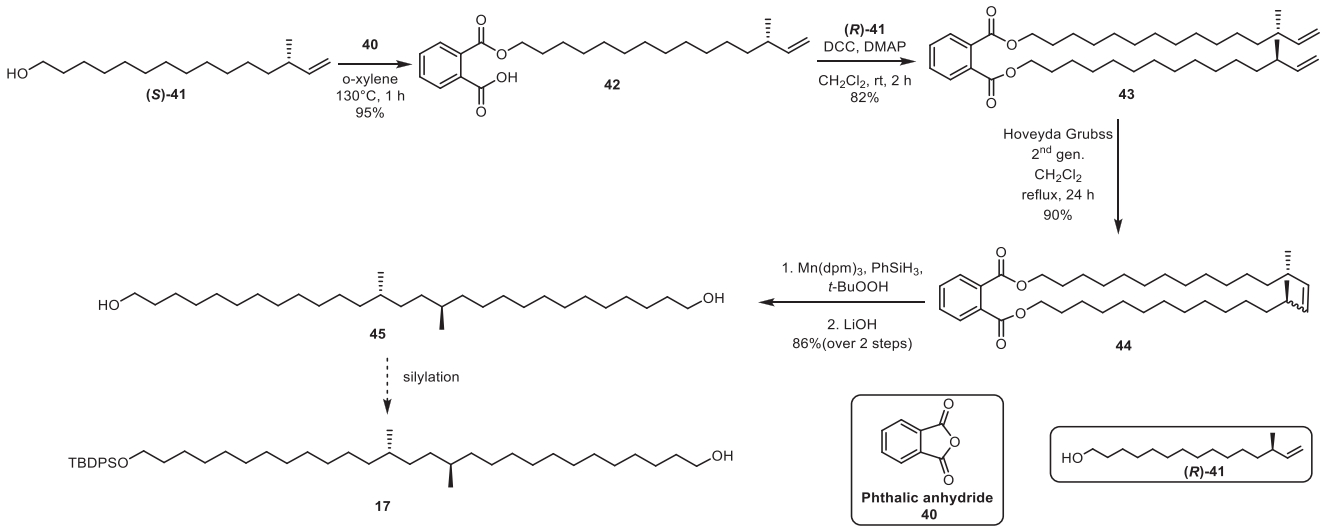

Scheme 6. Synthetic approach for anti-dimethyl **17**.

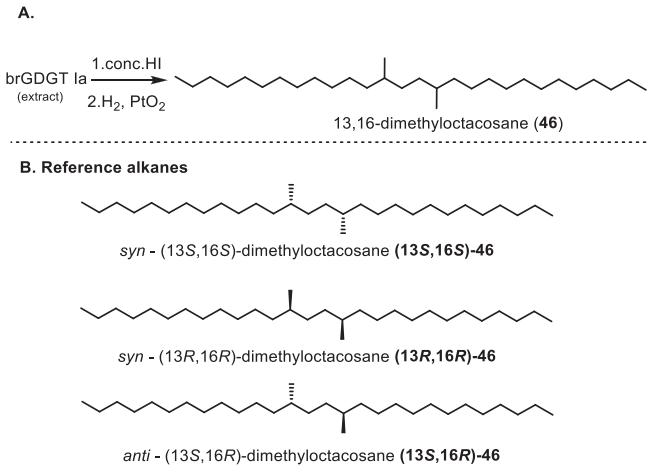

Scheme 7. (A) Synthesis of 13,16- dimethyl octacosane (**46**) from a lipid extract from *Solibacter usitatus*. (B) The reference alkanes **(13*S*,16*S*)-46**, **(13*R*,16*R*)-46**, and **(13*S*,16*R*)-46**.

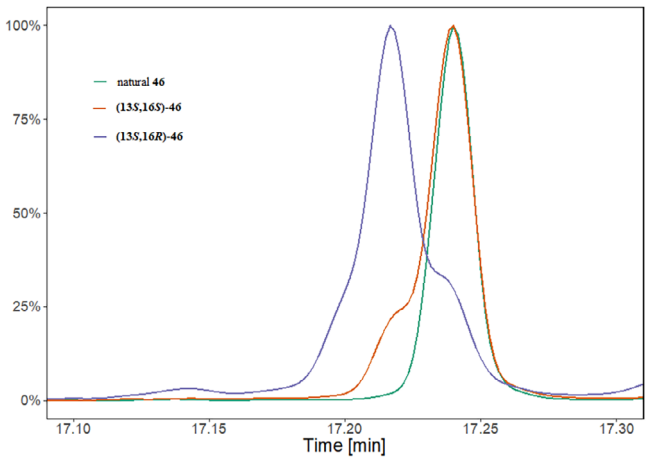

Figure 4. Overlay of the GC-FID chromatograms of the synthesized diastereomers of 13,16-dimethyloctacosane together with the one obtained from the natural extract. A DB-5HT column was used, with splitless injection at 375 °C and a temperature program starting at 40 °C going to 120 °C by 20 °C/min ramp, and then to 345 C by 15 C/min ramp. GC–FID temperature at 350 °C.

was subjected to ether cleavage with concentrated hydroiodic acid, resulting in the formation of the expected alkyl diiodides. Reduction with H_2/PtO_2 provided the corresponding 13,16-dimethyloctacosane (**46**) (Scheme 7).[43,44] To compare **46** obtained from the natural extract with synthetic reference compounds, the alkanes **(13*S*,16*S*)-46** and **(13*S*,16*R*)-46** were synthesized from their corresponding diols **27** and **45** using the HI and H_2/PtO_2 protocol. The other enantiomer with syn-configuration **(13*R*,16*R*)-46** was synthesized as well in the same way from the corresponding diol obtained in the synthesis of isomer **3B** of the lipid.

Upon analysis by GC-MS on a DB-5HT column, "natural" **46**, **(13*S*, 16*S*)-46** and **(13*S*,16*R*)-46** provided identical mass spectra, as expected (see Supporting Information). The chromatograms, however, revealed a small but notable difference in the retention time of the diastereomers **(13*S*,16*S*)-46** and **(13*S*,16*R*)-46**. An overlay of the chromatograms showed an overlap of the peak of **46** derived from the lipid extract of *Solibacter usitatus* with **(13*S*,16*S*)-46** (Figure 4). Therefore, we conclude beyond reasonable doubt that the relative configuration of the Me branches in brGDGT Ia (**3**) is "syn". Merging of the peaks of **(13*S*,16*S*)-46** and **(13*S*,16*R*)-46** at their base was observed in the overlay of their chromatograms. This shows that each of the synthetic isomers contains a small amount of their diastereomer. This results, as stated previously, from the 90% ee of the asymmetric alkylation step, forming 10% of the diastereomer after Grubbs metathesis.

Having established the overall structure of brGDGT Ia by chemical synthesis, including the relative configuration of the methyl-branched stereocenters, we finally made an attempt to determine the absolute configuration of the methyl-branched stereocenters. In addition to the comparison of natural brGDGT Ia (**3**) with both synthetic isomers **3A** and **3B** by HPLC, another promising route seemed to identify an enantio-separation of **46** by chiral GC. An HPLC comparison of the natural lipid with

its synthetic counterparts (**3A** and **3B**) with both normal and reversed-phase HPLC did however not provide any difference in retention time.

The enantio-separation of chiral alkanes by gas chromatography, despite or rather due to being challenging, has received considerable attention.[45–47] Unfortunately, though, we were despite many attempts not able to identify a chiral GC column that was able to achieve separation of synthesized enantiomers (**13*S*,16*S*)-46** and (**13*R*,16*R*)-46**. The attempts were in part thwarted by the high boiling point of **46**, whereas many chiral GC columns are restricted when it comes to high temperatures. This means that we have not been able to establish the absolute configuration of the methyl-branched stereocenters in 46 derived from natural lipid **3** by means of chiral chromatography, a challenge that is awaiting further progress in enantio-separation.

2.6. Elucidation of the Stereochemistry by VCD Spectroscopy

Considering the cryptochiral nature of **46**, any attempt to determine the absolute configuration of the alkanes by means of optical spectroscopies operating in the UV/vis range is likely to fail. Neither measurement of their optical rotations nor their circular dichroism (CD) spectra can be expected to yield reliable data (or none-zero spectra at all), as electronic transitions that give rise to these phenomena are lacking. Often being referred to as the chiral version of IR spectroscopy, vibrational circular dichroism (VCD) spectroscopy measures the difference in the absorbance of left- and right-circularly polarized infrared light by vibrational transitions. It thus does not rely on electronic transitions and is, in principle, applicable to any chiral molecule. Accordingly, it has also demonstrated its capabilities for the AC determination of cryptochiral molecules[48–50] such as 4-ethyl-4-methyloctane.[51] Nonetheless, purely aliphatic cryptochiral molecules present a particular challenge for VCD spectroscopy as they do not possess any polarized bonds and thus also show only weak IR activity. For the alkanes **46**, another particular challenge arises from the fairly long alkyl chains on both sides of the stereocenters. While their contributions to the VCD spectrum will mostly average out, they contribute to the IR absorbance spectrum. As concentrations need to be chosen such that total absorbance is avoided, the chiroptical information in the experimental VCD spectroscopic signatures will be notably weaker than for the aforementioned 4-ethyl-4-methyloctane.[51]

To explore whether it is at all possible to distinguish the antipodes, we recorded the experimental VCD and IR spectra of both enantiomers of **46** (Figure 5). We initially optimized the concentration of the sample so that we could capture the VCD signatures of the two strong IR bands at 1460 and 1375 cm^{-1}. While showing mirror image relation, the visual inspection of the experimental spectra gave the initial impression of them being of low quality. However, once it is acknowledged that the spectral features of **46** are extremely weak, it becomes apparent that this impression is related to the fact, that the spectra had to be expanded to the point that typically irrelevant noise and baseline imperfections became drastically amplified. Furthermore, the two strong IR bands used as a reference for the choice of the concentration of the sample actually turned out to not give particularly strong VCD bands, and the spectral range 1350–950 cm^{-1} was found to be much more informative. Unfortunately, as there was only a limited amount of sample available for the VCD studies, no further measurements at concentrations optimized for this lower wavenumber range could be carried out.

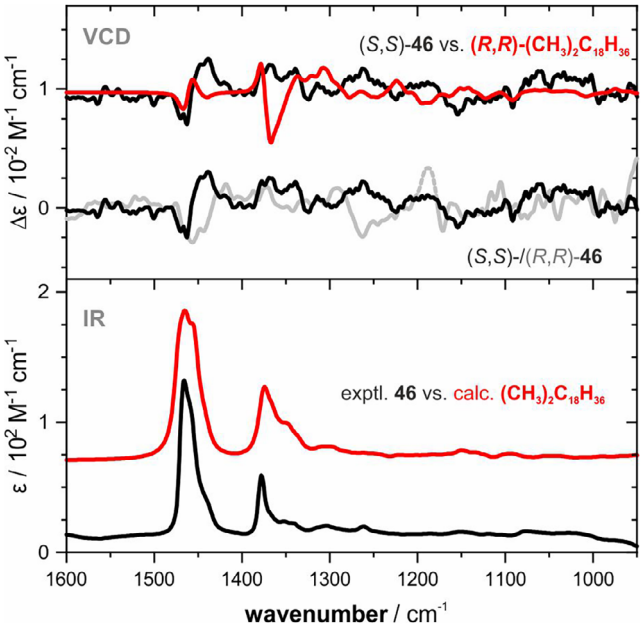

Figure 5. Experimental VCD (top) and IR spectra (bottom) of (**13*S*,16*S*)-46** (black, 0.8 M, 25 µm, $CDCl_3$) compared to the averaged VCD and IR spectra computed for (8*R*,11*R*)-dimethyloctadecane (red) and (**13*R*,16*R*)-46** (gray).

VCD and IR spectra calculations were carried out at the B3LYP/def2TZVP/IEFPCM($CHCl_3$) level of density functional theory (DFT).[52] Due to its large conformational space, the full length of the alkane **46** could not be considered in the calculations. Instead, the (*R*,*R*)-enantiomers of the truncated structures 3,6-dimethyloctane and 8,11-dimethyloctadecane were computed. For the simulation of the spectra of 8,11-dimethyloctadecane, we considered both Boltzmann-populations as well as a plain average over all single-conformer spectra. The latter approach accounts for the fact that linear, stretched conformers are favorable from the energetic perspective, but are less likely to be highly populated in the condensed phase. In Figure 5, the averaged VCD and IR spectra predicted for (8*R*,11*R*)-dimethyloctadecane are compared with the experimental spectrum of (**13*S*,16*S*)-46**. All other results are summarized in the Supporting Information. Despite the weak and noisy experimental signatures of **46**, the mirror-image relation with the computed VCD spectrum can clearly be seen especially for the signatures below 1400 cm^{-1}. A similar mirror image relation is observed for the enantiomers (**13*S*,16*S*)-46** and (**13*R*,16*R*)-46** (Figure 5). For the bands at 1460 and 1350 cm^{-1}, the match between computations and experiment is less satisfying. In these cases, however, it has to be considered that there is also a baseline artefact overlapping with the VCD bands, that obscures the band shapes.

Overall, it can thus be concluded that VCD spectroscopy can indeed distinguish the enantiomers of **46** and a computational analysis of the spectra is feasible. The key limitation for its application on the **46** derived from the natural extract of the lipid **3** thus remains to be the sample quantity required to record a spectrum, which in the present case amounted to 4–5 mg, and which should be notably increased in order to focus on the bands in the spectral range below 1350 cm^{-1}.

3. Conclusion

Stereoisomers of brGDGT Ia, **3A** and **3B** have been prepared in a linear sequence of 20 steps. The synthesis involved Cu-catalyzed asymmetric allylic alkylation to introduce the methyl-branched stereocenters and an effective KO*t*Bu/TBAB-mediated etherification reaction. These steps showed to be the cornerstones of a synthetic route that allowed the preparation of different diastereomers of the tetramethyl lipid and is expected to be suitable for the preparation of structurally similar branched GDGTs. The relative configuration of the 1,4-dimethyl unit in the chains was established to be "syn," whereas the absolute configuration of the methyl-branched stereocenters of the natural product remains to be defined. VCD spectroscopy has demonstrated its capabilities as a tool for assignment of absolute configuration, once experimental routines enable a drastic reduction of the required sample quantity and an optimized production route for the natural product. Establishing a synthetic route to obtain branched GDGTs with defined structure and purity aids a collaborative approach of both chemists and geochemists in paleoenvironmental studies and understanding the chemistry behind the evolution and biosynthesis of the lipids. The relative configuration of the methyl branches in brGDGTs being syn provides evidence for the involvement of similar enzymes in the biosynthesis of archaeal and branched GDGTs.[14–16]

Supporting Information

Experimental procedures and characterization data of all new compounds are provided in the supporting information. The authors have cited additional references within the Supporting Information.

Acknowledgements

The authors acknowledge European Union's Horizon 2020 research and innovation programme under Grant Agreement No. 847675 for funding the COFUND project oLife (oLife postdoctoral fellowship), and an NSF CAREER grant (EAR1945484) for funding *S. usitatus* research. This work was further funded by the Deutsche Forschungsgemeinschaft (DFG, German Research Foundation) under Germany's Excellence Strategy (EXC-2033, project no. 390677874). The authors thank M. T. Todosia, and R. Tarozo, Stratingh Institute for Chemistry, University of Groningen. Prof. U. Meierhenrich (University of Côte d'Azur) is acknowledged for support in chiral separation. H. Allbrook, J. Sepúlveda, X. Liu, and the CU Boulder Earth Systems Stable Isotope Lab (Core facility RRID:SCR_019300) for their respective analytical contributions.

Conflict of Interest

The authors declare no conflict of interest.

Data Availability Statement

The data that support the findings of this study are available in the Supporting Information of this article.

Keywords: asymmetric synthesis · branched tetraethers · relative configuration · stereoisomers · total synthesis

[1] C. R. Woese, G. E. Fox, *Proc. Natl. Acad. Sci.* **1977**, *74*, 5088.
[2] C. R. Woese, *Proc. Natl. Acad. Sci. U. S. A.* **1990**, *87*, 4576.
[3] Y. Koga, M. Nishihara, H. Morii, M. Akagawa-Matsushita, *Microbiol. Rev.* **1993**, *57*, 164.
[4] M. Kates, *Prog. Chem. Fats Other Lipids* **1977**, *15*, 301.
[5] J. Lombard, P. López-García, D. Moreira, *Nat. Rev. Microbiol.* **2012**, *10*, 507.
[6] H. Hirschmann, *J. Biol. Chem.* **1960**, *235*, 2762.
[7] Y. Koga, *J. Mol. Evol.* **2011**, *72*, 274.
[8] Y. Koga, *J. Mol. Evol.* **2014**, *78*, 234.
[9] L. Villanueva, S. Schouten, J. S. S. Damsté, *Environ. Microbiol.* **2017**, *19*, 54.
[10] Y. Koga, *Archaea* **2012**, *2012*, 789652.
[11] J. S. S. Damsté, E. C. Hopmans, R. D. Pancost, S. Schouten, J. A. J. Geenevasen, *Chem. Commun.* **2000**, 1683.
[12] J. W. H. Weijers, S. Schouten, E. C. Hopmans, J. A. J. Geenevasen, O. R. P. David, J. M. Coleman, R. D. Pancost, J. S. Sinninghe Damsté, *Environ. Microbiol.* **2006**, *8*, 648.
[13] C. T. Lloyd, D. F. Iwig, B. Wang, M. Cossu, W. W. Metcalf, A. K. Boal, S. J. Booker, *Nature* **2022**, *609*, 197.
[14] Z. Zeng, H. Chen, H. Yang, Y. Chen, W. Yang, X. Feng, H. Pei, P. V. Welander, *Nat. Commun.* **2022**, *13*, 1545.
[15] J. S. Sinninghe Damsté, W. I. C. Rijpstra, E. C. Hopmans, J. W. H. Weijers, B. U. Foesel, J. Overmann, S. N. Dedysh, *Appl. Environ. Microbiol.* **2011**, *77*, 4147.
[16] D. X. Sahonero-Canavesi, M. F. Siliakus, A. Abdala Asbun, M. Koenen, F. A. B. Von Meijenfeldt, S. Boeren, N. J. Bale, J. C. Engelman, K. Fiege, L. Strack Van Schijndel, J. S. Sinninghe Damsté, L. Villanueva, *Sci. Adv.* **2022**, *8*, eabq8652.
[17] V. Torsvik, L. Øvreås, T. F. Thingstad, *Science* **2002**, *296*, 1064.
[18] J. W. H. Weijers, E. Panoto, J. Van Bleijswijk, S. Schouten, W. I. C. Rijpstra, M. Balk, A. J. M. Stams, J. S. S. Damsté, *Geomicrobiol. J.* **2009**, *26*, 402.
[19] J. W. H. Weijers, G. L. B. Wiesenberg, R. Bol, E. C. Hopmans, R. D. Pancost, *Biogeosciences* **2010**, *7*, 2959.
[20] T. A. Halamka, J. H. Raberg, J. M. McFarlin, A. D. Younkin, C. Mulligan, X. Liu, S. H. Kopf, *Geobiology* **2023**, *21*, 102.
[21] Y. Chen, F. Zheng, H. Yang, W. Yang, R. Wu, X. Liu, H. Liang, H. Chen, H. Pei, C. Zhang, R. D. Pancost, Z. Zeng, *Geochim. Cosmochim. Acta* **2022**, *337*, 155.
[22] F. Peterse, J. Van Der Meer, S. Schouten, J. W. H. Weijers, N. Fierer, R. B. Jackson, J.-H. Kim, J. S. Sinninghe Damsté, *Geochim. Cosmochim. Acta* **2012**, *96*, 215.
[23] C. De Jonge, D. Radujković, B. D. Sigurdsson, J. T. Weedon, I. Janssens, F. Peterse, *Org. Geochem.* **2019**, *137*, 103897.
[24] B. D. A. Naafs, G. N. Inglis, Y. Zheng, M. J. Amesbury, H. Biester, R. Bindler, J. Blewett, M. A. Burrows, D. Del Castillo Torres, F. M. Chambers,

A. D. Cohen, R. P. Evershed, S. J. Feakins, M. Gałka, A. Gallego-Sala, L. Gandois, D. M. Gray, P. G. Hatcher, E. N. Honorio Coronado, P. D. M. Hughes, A. Huguet, M. Könönen, F. Laggoun-Défarge, O. Lähteenoja, M. Lamentowicz, R. Marchant, E. McClymont, X. Pontevedra-Pombal, C. Ponton, A. Pourmand, et al., *Geochim. Cosmochim. Acta* **2017**, *208*, 285.
[25] B. D. A. Naafs, A. V. Gallego-Sala, G. N. Inglis, R. D. Pancost, *Org. Geochem.* **2017**, *106*, 48.
[26] J. S. Sinninghe Damsté, W. I. C. Rijpstra, B. U. Foesel, K. J. Huber, J. Overmann, S. Nakagawa, J. J. Kim, P. F. Dunfield, S. N. Dedysh, L. Villanueva, *Org. Geochem.* **2018**, *124*, 63.
[27] S. Schouten, E. C. Hopmans, E. Schefuß, J. S. Sinninghe Damsté, *Earth Planet. Sci. Lett.* **2002**, *204*, 265.
[28] J. W. H. Weijers, S. Schouten, J. C. Van Den Donker, E. C. Hopmans, J. S. Sinninghe Damsté, *Geochim. Cosmochim. Acta* **2007**, *71*, 703.
[29] E. C. Hopmans, J. W. H. Weijers, E. Schefuß, L. Herfort, J. S. Sinninghe Damsté, S. Schouten, *Earth Planet. Sci. Lett.* **2004**, *224*, 107.
[30] S. Schouten, E. C. Hopmans, A. Rosell-Melé, A. Pearson, P. Adam, T. Bauersachs, E. Bard, S. M. Bernasconi, T. S. Bianchi, J. J. Brocks, L. T. Carlson, I. S. Castañeda, S. Derenne, A. D. Selver, K. Dutta, T. Eglinton, C. Fosse, V. Galy, K. Grice, K. Hinrichs, Y. Huang, A. Huguet, C. Huguet, S. Hurley, A. Ingalls, G. Jia, B. Keely, C. Knappy, M. Kondo, S. Krishnan, et al., *Geochem. Geophys. Geosystems* **2013**, *14*, 5263.
[31] X.-L. Liu, D. A. Russell, C. Bonfio, R. E. Summons, *Org. Geochem.* **2019**, *128*, 57.
[32] R. L. H. Andringa, N. A. W. Kok, A. J. M. Driessen, A. J. Minnaard, *Angew. Chem., Int. Ed.* **2021**, *60*, 17497.
[33] I. D. Falk, B. Gál, A. Bhattacharya, J. H. Wei, P. V. Welander, S. G. Boxer, N. Z. Burns, *Angew. Chem., Int. Ed.* **2021**, *60*, 17491.
[34] F. Saito, P. R. Schreiner, *Eur. J. Org. Chem.* **2020**, *2020*, 6328.
[35] M. Holzheimer, J. S. Sinninghe Damsté, S. Schouten, R. W. A. Havenith, A. V. Cunha, A. J. Minnaard, *Angew. Chem., Int. Ed.* **2021**, *60*, 17504.
[36] F. López, A. W. Van Zijl, A. J. Minnaard, B. L. Feringa, *Chem. Commun.* **2006**, 409.
[37] D. Geerdink, B. T. Horst, M. Lepore, L. Mori, G. Puzo, A. K. H. Hirsch, M. Gilleron, G. De Libero, A. J. Minnaard, *Chem. Sci.* **2013**, *4*, 709.
[38] T. Ireland, G. Grossheimann, C. Wieser-Jeunesse, P. Knochel, *Angew. Chem., Int. Ed.* **1999**, *38*, 3212.
[39] T. Ireland, G. Grossheimann, C. Wieser-Jeunesse, P. Knochel, *Angew. Chem., Int. Ed.* **2008**, *47*, 3666.
[40] M. Tsuda, T. Endo, J. Kobayashi, *J. Org. Chem.* **2000**, *65*, 1349.
[41] M. Tsuda, Y. Toriyabe, T. Endo, J. Kobayashi, *Chem. Pharm. Bull.* **2003**, *51*, 448.
[42] K. Iwasaki, K. K. Wan, A. Oppedisano, S. W. M. Crossley, R. A. Shenvi, *J. Am. Chem. Soc.* **2014**, *136*, 1300.
[43] M. Kaneko, F. Kitajima, H. Naraoka, *Org. Geochem.* **2011**, *42*, 166.
[44] W. D. Leavitt, S. H. Kopf, Y. Weber, B. Chiu, J. M. McFarlin, F. J. Elling, S. Hoeft-McCann, A. Pearson, *Geochim. Cosmochim. Acta* **2023**, *352*, 194.
[45] U. J. Meierhenrich, M.-J. Nguyen, B. Barbier, A. Brack, W. H.-P. Thiemann, *Chirality* **2003**, *15*, S13.
[46] G. Leseigneur, J.-J. Filippi, N. Baldovini, U. Meierhenrich, *Symmetry* **2022**, *14*, 326.
[47] K. Huang, D. W. Armstrong, *Org. Geochem.* **2009**, *40*, 283.
[48] C. Merten, T. P. Golub, N. M. Kreienborg, *J. Org. Chem.* **2019**, *84*, 8797.
[49] A. Masarwa, D. Gerbig, L. Oskar, A. Loewenstein, H. P. Reisenauer, P. Lesot, P. R. Schreiner, I. Marek, *Angew. Chem., Int. Ed.* **2015**, *54*, 13106.
[50] P. R. Schreiner, A. A. Fokin, H. P. Reisenauer, B. A. Tkachenko, E. Vass, M. M. Olmstead, D. Bläser, R. Boese, J. E. P. Dahl, R. M. K. Carlson, *J. Am. Chem. Soc.* **2009**, *131*, 11292.
[51] S. Kuwahara, K. Obata, T. Fujita, N. Miura, A. Nakahashi, K. Monde, N. Harada, *Eur. J. Org. Chem.* **2010**, *2010*, 6385.
[52] M. J. Frisch, G. W. Trucks, H. B. Schlegel, G. E. Scuseria, M. A. Robb, J. R. Cheeseman, G. Scalmani, V. Barone, B. Mennucci, G. A. Petersson, H. Nakatsuji, M. Caricato, X. Li, H. P. Hratchian, A. F. Izmaylov, J. Bloino, G. Zheng, J. L. Sonnenberg, M. Hada, M. Ehara, K. Toyota, R. Fukuda, J. Hasegawa, M. Ishida, T. Nakajima, Y. Honda, O. Kitao, H. Nakai, T. Vreven, J. J. A. Montgomery, et al., *Gaussian 09, Rev E.01*, Wallingford CT, USA **2013**.

Manuscript received: February 23, 2025
Revised manuscript received: March 11, 2025
Version of record online: March 29, 2025